JOURNAL OF GUIDANCE, CONTROL, AND DYNAMICS
Vol. 32, No. 3, May–June 2009

Stabilization of Collective Motion in a Time-Invariant Flowfield

Derek A. Paley* and Cameron Peterson†
University of Maryland, College Park, Maryland 20742

DOI: 10.2514/1.40636

Cooperative steering controls enable mobile sampling platforms to conduct synoptic, adaptive surveys of dynamic spatiotemporal processes by appropriately regulating the space-time separation of their sampling trajectories. Sensing platforms in the air and maritime domains can be pushed off course by strong and variable environmental dynamics. However, most existing cooperative-control algorithms are based on simple motion models that do not include a flowfield. Existing models that include the flowfield often include speed control to compensate for the flow. In this paper, we describe a constant-speed self-propelled particle model that explicitly incorporates a time-invariant flowfield. Each vehicle is represented by a Newtonian particle subject to a gyroscopic steering control. We describe the Lyapunov-based design of decentralized control algorithms that stabilize collective motion in a known flowfield. In the case of a spatially variable flow, we provide an algorithm to stabilize synchronized motion, in which all of the particles move in the same direction, and circular motion, in which all of the particles orbit an inertially fixed point at a constant radius. For a spatially invariant flow, we provide an algorithm to stabilize balanced motion, in which the particle position centroid is inertially fixed, and symmetric circular formations, in which the particle spacing around a circle is temporally regulated. Via the latter algorithm, we provide a method of stabilizing a circular formation in which the particles are evenly spaced in time and the formation is centered on a moving target. The theoretical results are illustrated with two numerical examples based on applications in environmental monitoring and target surveillance.

Nomenclature

c_k	=	center of circle traversed by particle k
f_k	=	flow velocity at position r_k
i	=	imaginary unit
K	=	control gain
N	=	number of particles
P	=	$N \times N$ projector matrix
P_k	=	kth row of matrix P
r_k	=	position of particle k
$\dot{r}_k$	=	inertial velocity of particle k
s_k	=	speed of particle k
T	=	period of revolution around a circular orbit
γ_k	=	orientation of the inertial velocity of particle k
θ_k	=	orientation of the velocity of particle k relative to the flow
ψ_k	=	time phase of particle k in a circular orbit
ω_0	=	constant angular rate

Subscripts

j, k	=	particle and phase indices, $1, \ldots, N$

I. Introduction

AUTONOMOUS vehicles provide a robust sensing platform for synoptic and adaptive sampling of spatiotemporal processes in the air and sea. Decentralized control algorithms that coordinate the sampling trajectories of multiple vehicles enhance the sensory performance of the entire fleet by appropriately regulating the space-time separation of sample points [1]. A major impediment to the regulation of trajectory separation is the presence of an external flowfield (e.g., ocean currents or atmospheric winds). Cooperative-control algorithms that are effective in weak flowfields often fail in moderate to strong flows. In this paper, we provide decentralized algorithms that stabilize collective motion in a time-invariant flowfield. We assume that 1) the flowfield is known and 2) the flowfield is weaker than the particle speed relative to the flow, although these theoretical restrictions have been successfully lifted in numerical simulations. The extension of the theoretical results to strong and variable flows is the subject of ongoing analysis.

Robust coordination of multiple vehicles in the absence of flow can be produced by cooperative control of a dynamic motion model in which each vehicle is represented by a Newtonian particle moving at constant speed in a plane [2–4]. Each particle is subject to a gyroscopic (steering) control that determines the rate of rotation of the particle velocity. Using a particle framework, theoretically justified algorithms [5,6] generate symmetric formations in which the relative positions and relative orientations of all vehicles are optimized for sampling performance (under very mild assumptions on the intervehicle communication). These algorithms have been successfully demonstrated in multiple at-sea experiments with autonomous underwater vehicles [7,8].

Analysis of ocean-sampling field experiments highlights the need to develop theoretically justified algorithms that stabilize collective motion in the presence of a strong and variable flowfield [9]. Underwater vehicles routinely encounter ocean currents that match or exceed vehicle speed. These currents push vehicles away from their desired trajectories and compress/expand the space-time separation of vehicle trajectories, leading to a degradation of overall sampling performance. Strong currents that vary substantially in time are especially challenging because of the inherent uncertainty in current forecasts. The derivation of cooperative-control and estimation algorithms for strong and variable currents is outside the scope of this paper. We focus instead on what to do in the presence of a known, time-invariant flow in which an underwater or aerial vehicle has strictly positive speed-over-ground.

We use a planar model that explicitly incorporates a time-invariant flowfield [10,11]. Each vehicle is represented by a Newtonian particle subject to a gyroscopic steering control. We present a Lyapunov-based design of decentralized control algorithms that stabilize collective motion in a known flowfield. The control design is a direct extension of the framework introduced for the flow-free model with all-to-all communication [5]. Accordingly, all of the

Received 27 August 2008; revision received 26 November 2008; accepted for publication 28 November 2008.

*Assistant Professor, Department of Aerospace Engineering; dpaley@umd.edu. Senior Member AIAA.

†Graduate Student, Department of Aerospace Engineering; cammykai@yahoo.com.

results presented herein extend naturally to limited communication topologies that may be time varying and/or directed [6]. Likewise, our focus on parallel and circular motion is for brevity only; the framework has been extended to motion on convex loops in a flowfield [12].

In the case of a spatially variable flow, we provide an algorithm to stabilize synchronized motion, in which all of the particles move in the same direction, and circular motion, in which all of the particles orbit an inertially fixed point at a constant radius. In addition, we show how to prescribe the center of a circular formation using a virtual particle. For a spatially invariant flow, we provide an algorithm to stabilize balanced motion, in which the particle position centroid is inertially fixed, and symmetric circular formations, in which the particle spacing around a circle is temporally regulated. Via the latter algorithm, we provide a method of stabilizing a circular formation in which the particles are evenly spaced in time. These motion primitives collectively form a foundation upon which more complex mission-specific trajectories can be constructed.

The results presented here contribute to a body of research results that highlight the impact of a flowfield on motion planning for unmanned vehicles [13–17]. For example, it has been shown that, unlike in the no-wind case, the minimum time paths in wind from a known start point to a known endpoint consist of three arcs [14]. Furthermore, onboard-camera tilt and pan are minimized in wind by an elliptical platform trajectory that spirals in toward a target [16]. We provide control laws to stabilize a circular formation centered on an inertially fixed point: results that are applicable to stabilizing a formation of constant-speed vehicles to a circular orbit centered on a target moving at a constant velocity [18–20]. An alternate algorithm exists to match the average vehicle velocity to a time-invariant reference and, with the use of an outer-loop control, to a known time-varying reference [18].

The problem of tracking a moving target with a circular formation of variable-speed vehicles has also been studied recently [21,22]. The trajectory of a vehicle can be controlled through Lyapunov guidance vector fields chosen to satisfy a specific candidate Lyapunov function and thereby provide globally stable paths [21]. Guidance vector fields containing a limit cycle allow multiple vehicles to orbit a constant-velocity target at a desired standoff radius. For vehicles without speed control traveling in a circular formation in wind, only regulation of temporal and not spatial separation is possible. The notion of temporal regulation of constant-speed vehicles in a circular formation has been studied in the context of a sliding-mode design of a solution to the target-tracking problem in which multiple vehicles orbit a target at regular intervals [20]. We further explore this notion, using our control design concepts from the literature on cooperative control via coupled phase oscillator models [5,6].

The paper has the following outline. In Sec. II, we describe a self-propelled particle model that explicitly incorporates a time-invariant flowfield. In Sec. III, we provide decentralized control algorithms to stabilize, respectively, a synchronized formation in a spatially variable field and a balanced formation in a spatially invariant field. In Sec. IV, we provide an algorithm to stabilize a circular formation in a spatially variable field. In Sec. V, we provide algorithms to isolated circular formations in which the temporal separation of particles in the formation is temporally regulated in a spatially invariant field. In Sec. VI, we provide results from numerical simulations related to applications in environmental monitoring and target surveillance. In Sec. VII, we summarize the results and provide indications of ongoing and future work, which includes the stabilization of collective motion in a time-varying flowfield.

II. Model of Particles in a Flowfield

In this paper, we study a dynamic model of N self-propelled particles in a time-invariant flowfield. Each particle is subject to a steering control produced by a gyroscopic force that remains normal to the particle velocity relative to the flow. The position of the kth particle is denoted by r_k, where $k \in \{1, \ldots, N\}$, and the inertial velocity of the kth particle is denoted by $\dot{r}_k$, as illustrated in Fig. 1. Let

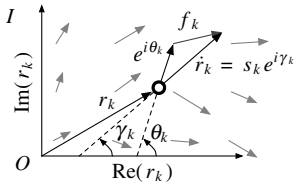

Fig. 1 Particles move at unit speed relative to a time-invariant flowfield.

$\mathcal{I}$ denote an inertial reference frame with origin O. Each particle propels itself relative to the flow at unit speed[‡] in the direction θ_k, which is measured relative to the positive, horizontal axis of $\mathcal{I}$. In complex notation, the velocity of particle k relative to the flow is denoted $\cos\theta_k + i\sin\theta_k = e^{i\theta_k}$. We represent the inertial velocity of the flow at r_k by $f_k = f(r_k)$. We assume that the flowfield is known, time-invariant, and satisfies $|f_k| < 1$. (The latter assumption ensures that a particle can always make forward progress as measured in an inertial frame.) Except where specified, the flowfield is permitted to be spatially variable (nonuniform) as long as it is continuously differentiable and $f'_k = \partial f_k / \partial r_k$ is known for all r_k.

The equations of motion of the particle model are

$$\dot{r}_k = e^{i\theta_k} + f_k \qquad \dot{\theta}_k = u_k \tag{1}$$

where the steering control u_k is determined by a decentralized state feedback law. To maintain our focus on the novel contributions of this paper, we assume an all-to-all communication topology. Nonetheless, the framework is easily extended to limited communication topologies following a development identical to the flow-free model [5,6].

Let γ_k denote the orientation of the inertial velocity of particle k and $s_k = s(r_k, \gamma_k)$ denote its magnitude. That is, let $\dot{r}_k = s_k e^{i\gamma_k}$, where $s_k = |e^{i\theta_k} + f_k|$ and $\gamma_k = \arg(e^{i\theta_k} + f_k)$. Note $|s_k| \geq |1 - |f_k|| > 0$, by assumption. From Fig. 1, we have[§]

$$s_k \sin\gamma_k = \sin\theta_k + \langle f_k, i\rangle \tag{2}$$

$$s_k \cos\gamma_k = \cos\theta_k + \langle f_k, 1\rangle \tag{3}$$

or, equivalently,

$$\sin\theta_k = s_k \sin\gamma_k - \langle f_k, i\rangle \tag{4}$$

$$\cos\theta_k = s_k \cos\gamma_k - \langle f_k, 1\rangle \tag{5}$$

which imply

$$\tan\gamma_k = \frac{\sin\theta_k + \langle f_k, i\rangle}{\cos\theta_k + \langle f_k, 1\rangle} \tag{6}$$

Differentiating Eq. (6) with respect to time along solutions of Eq. (1) and solving for $\dot{\gamma}_k$ using Eqs. (4) and (5), we obtain

$$\dot{\gamma}_k = (\cos\theta_k \cos\gamma_k + \sin\theta_k \sin\gamma_k) s_k^{-1} \dot{\theta}_k + \langle \dot{f}_k, i\rangle s_k^{-1} \cos\gamma_k - \langle \dot{f}_k, 1\rangle s_k^{-1} \sin\gamma_k = (1 - s_k^{-1}\langle e^{i\gamma_k}, f_k\rangle) u_k + \langle \dot{f}_k, i e^{i\gamma_k}\rangle s_k^{-1} \triangleq \nu_k \tag{7}$$

where $\dot{f}_k = f'_k \dot{r}_k$.

We view ν_k defined in Eq. (7) as a control input, because one can compute u_k according to

$$u_k = \frac{\nu_k - \langle f'_k, i\rangle}{1 - s_k^{-1}\langle e^{i\gamma_k}, f_k\rangle} \tag{8}$$

[‡]The flow speeds used in this paper can be interpreted as the absolute flow speed divided by the platform speed relative to the flow.

[§]We use the inner product $\langle x, y\rangle = \mathrm{Re}\{\bar{x}y\}$, where $x, y \in \mathbb{C}$ and $\bar{x}$ is the complex conjugate of x.

Note that Eq. (8) is well defined because the denominator is never equal to zero. We prove this fact by contradiction. Suppose the denominator is equal to zero, then

$$s_k = \langle e^{i\gamma_k}, f_k \rangle = \langle e^{i\theta_k} + f_k, f_k \rangle s_k^{-1} \tag{9}$$

which implies

$$s_k^2 = \langle e^{i\theta_k} + f_k, e^{i\theta_k} + f_k \rangle = \langle e^{i\theta_k} + f_k, f_k \rangle \tag{10}$$

and, after canceling terms,

$$1 + \langle e^{i\theta_k}, f_k \rangle = 0 \tag{11}$$

However, Eq. (11) is a contradiction because $|\langle e^{i\theta_k}, f_k \rangle| \leq |f_k| < 1$, by assumption.

As a consequence of this analysis, it is equivalent to write Eq. (1) as

$$\dot{r}_k = s_k e^{i\gamma_k} \qquad \dot{\gamma}_k = \nu_k \tag{12}$$

where ν_k is defined in Eq. (7). The model (12) is a self-propelled particle model with a variable speed $s_k = |e^{i\theta_k} + f_k| > 0$ and steering control ν_k. Note, the speed s_k depends on the particle phase γ_k and, possibly, the position r_k; the speed s_k is not a control variable.

In the following two examples, we calculate s_k and u_k for a uniform flow and a nonuniform flow, respectively.

Example 1, uniform flow: Without loss of generality, we align the positive real axis of the inertial frame with the orientation of a uniform flow, so that $f_k = \beta \in \mathbb{R}$, $|\beta| < 1$. We calculate

$$s_k = \sqrt{\mathrm{Re}\{(\beta + e^{i\theta_k})(\beta + e^{-i\theta_k})\}} = \sqrt{1 + \beta^2 + 2\beta\cos\theta_k} \tag{13}$$

We express s_k as a function of γ_k and $f_k = \beta$ by substituting Eq. (5) into Eq. (13) and rearranging the result to obtain the quadratic equation

$$s_k^2 - 2\beta\cos\gamma_k s_k + \beta^2 - 1 = 0$$

which has the solution (using the positive root since $s_k > 0$)

$$s_k = \beta\cos\gamma_k + \sqrt{1 - \beta^2\sin^2\gamma_k} \tag{14}$$

Note, s_k for a uniform flowfield is a function of γ_k only, and not r_k. To find u_k as a function of ν_k, substitute $f_k = \beta$ (and $f_k' = 0$) into Eq. (8) to obtain

$$u_k = \frac{\nu_k}{1 - \beta s_k^{-1}\cos\gamma_k} \tag{15}$$

Example 2, nonuniform flow: Let $f_k = \beta_k + i\alpha_k$, where $\beta_k = \langle f_k, 1 \rangle$ and $\alpha_k = \langle f_k, i \rangle$ are the real and imaginary parts, respectively, of a spatially variable flowfield. We have

$$\begin{aligned} s_k &= \sqrt{\mathrm{Re}\{(e^{i\theta_k} + \beta_k + i\alpha_k)(e^{-i\theta_k} + \beta_k - i\alpha_k)\}} \\ &= \sqrt{1 - \beta_k^2 - \alpha_k^2 + 2s_k(\alpha_k\sin\gamma_k + \beta_k\cos\gamma_k)} \end{aligned} \tag{16}$$

where we used Eqs. (4) and (5). Squaring both sides of Eq. (16) and solving the resulting quadratic equation (using the positive root since $s_k > 0$) yields

$$\begin{aligned} s_k &= \alpha_k\sin\gamma_k + \beta_k\cos\gamma_k + \sqrt{1 - (\alpha_k\cos\gamma_k - \beta_k\sin\gamma_k)^2} \\ &= \langle e^{i\gamma_k}, f_k \rangle + \sqrt{1 - \langle ie^{i\gamma_k}, f_k \rangle^2} \end{aligned} \tag{17}$$

Note, s_k depends here on both γ_k and r_k.

To compute u_k for a nonuniform flowfield, let $r_k = x_k + iy_k$, which implies

$$\dot{f}_k = \frac{\partial\beta}{\partial x_k}\dot{x}_k + \frac{\partial\beta}{\partial y_k}\dot{y}_k + i\left(\frac{\partial\alpha}{\partial x_k}\dot{x}_k + \frac{\partial\alpha}{\partial y_k}\dot{y}_k\right) \tag{18}$$

Substituting Eq. (18) into Eq. (8) completes the calculation. In the simulations in Secs. III and IV, we use a smooth, periodic flowfield

$$f_k = a_0\sin(2\pi\omega x_k - \varphi_0) + i\cos(2\pi\omega y_k - \varphi_0) \tag{19}$$

which is parametrized by a_0, ω, and φ_0.

III. Phase Synchronization and Balancing

Three motion primitives of the particle model (12) illustrated in Fig. 2 are synchronized, balanced, and circular motions [5]. In this section, we study synchronized and balanced motions and, in the next section, we study circular motions. In synchronized motion, all of the phases $\gamma_k, k = 1, \ldots, N$, are equal and the particles move in the same direction with arbitrary separation. In balanced motion, the centroid of the particle positions

$$p_r \triangleq \frac{1}{N}\sum_{j=1}^{N} r_j$$

is fixed, which implies that the quantity

$$p_{\dot{r}} \triangleq \frac{1}{N}\sum_{j=1}^{N} \dot{r}_j = \dot{p}_r$$

is zero. A Lyapunov-based control framework exists to stabilize synchronized and balanced motions in a flow-free particle model [5]. In this section, we extend the flow-free framework to stabilize synchronized and balanced motions in a time-invariant flowfield.

Synchronized motion corresponds to the maximum of the potential[¶]

$$U(\boldsymbol{\gamma}) \triangleq \tfrac{1}{2}|p_\gamma|^2 \tag{20}$$

where

$$p_\gamma \triangleq \frac{1}{N}\sum_{j=1}^{N} e^{i\gamma_j} \tag{21}$$

is the centroid of the phasors $e^{i\gamma_k}, k = 1, \ldots, N$. The following result is proven using Lyapunov stability theory.

Theorem 1: The closed-loop particle model (12) with the gradient control

$$\nu_k = -K\frac{\partial U}{\partial\gamma} = -K\langle p_\gamma, ie^{i\gamma_k} \rangle, \qquad K < 0 \tag{22}$$

forces convergence of all solutions to the critical set of U. The set of synchronized motions are asymptotically stable and every other equilibrium is unstable.

Proof: See [5], Theorem 1. □

We illustrate Theorem 1 in Fig. 3. Note, the arrow attached to each particle represents its velocity relative to the flow. The nonuniform flow is generated by Eq. (19) with $a_0 = -0.75$, $\omega = 1/360$, and $\varphi_0 = 10$.

Theorem 1 provides a decentralized synchronization algorithm for a nonuniform flowfield. To stabilize balanced motions, we assume that the flow is uniform (see Example 1). We stabilize balanced solutions of Eq. (12) with $f_k = \beta \in \mathbb{R}$ by minimizing the potential [10]

$$V(\boldsymbol{r}, \boldsymbol{\gamma}) = \tfrac{1}{2}|p_{\dot{r}}|^2 \tag{23}$$

where

$$p_{\dot{r}} \triangleq \frac{1}{N}\sum_{j=1}^{N} s_j e^{i\gamma_j} \tag{24}$$

[¶]We drop the subscript and use bold to represent an $N \times 1$ matrix, for example, $\gamma = (\gamma_1, \ldots, \gamma_N)^T$.

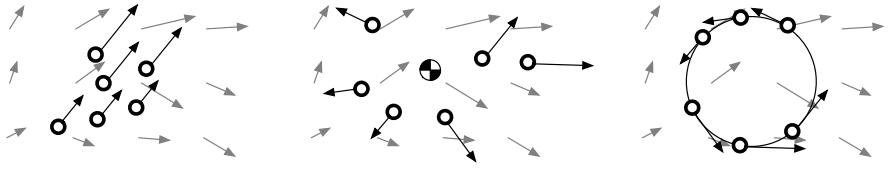

a) Synchronized motion **b) Balanced motion** **c) Circular motion**

Fig. 2 Three motion primitives of the particle model in a time-invariant flowfield.

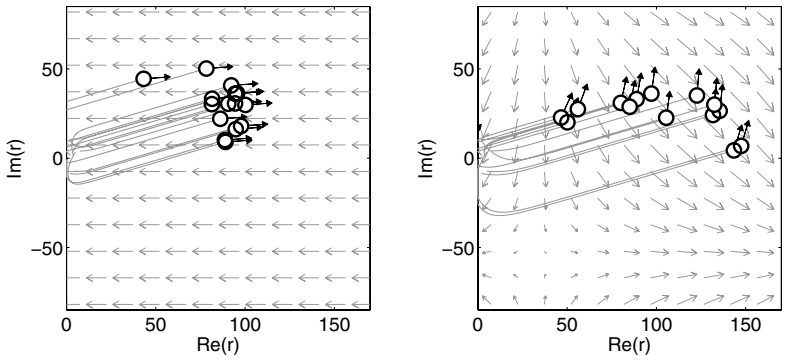

a) Uniform flow, β=−0.75 **b) Nonuniform flow in Eq. (19)**

Fig. 3 Synchronization of particle phases using control (22) with $N = 15$ and $K = -0.1$.

is the centroid of the particle velocities. Note $V(\boldsymbol{r}, \boldsymbol{\gamma}) = 0$ when $p_{\dot{r}} = 0$, that is, the centroid of particle positions is fixed, and positive otherwise. The time derivative of $V(\boldsymbol{r}, \boldsymbol{\gamma})$ along solutions of Eq. (12) is

$$\dot{V} = \langle p_{\dot{r}}, \dot{p}_{\dot{r}} \rangle = \sum_{j=1}^{N} \langle p_{\dot{r}}, \dot{s}_j e^{i\gamma_j} + s_j i e^{i\gamma_j} \dot{\gamma}_j \rangle \tag{25}$$

where, for a uniform flow,

$$\dot{s}_k = \delta_k s_k \dot{\gamma}_k, \qquad \delta_k \triangleq \frac{-\beta \sin \gamma_k}{\sqrt{1 - \beta^2 \sin^2 \gamma_k}} \tag{26}$$

Substituting Eq. (26) into Eq. (25) yields

$$\dot{V} = \sum_{j=1}^{N} \langle p_{\dot{r}}, (\delta_j + i) e^{i\gamma_j} \rangle s_j \nu_j \tag{27}$$

Lyapunov analysis leads to the following result.

Theorem 2: The particle model (12) with $f_k = \beta$, $|\beta| < 1$, and the control

$$\nu_k = -K \langle p_{\dot{r}}, (\delta_k + i) e^{i\gamma_k} \rangle s_k, \qquad K > 0 \tag{28}$$

where δ_k is defined in Eq. (26), asymptotically stabilizes the set of balanced motions, which is the set of motions for which the centroid of particle positions is fixed.

Proof: Substituting Eq. (28) into Eq. (27) yields

$$\dot{V} = -K \sum_{j=1}^{N} \langle p_{\dot{r}}, (\delta_j + i) e^{i\gamma_j} \rangle^2 s_j^2 \leq 0 \tag{29}$$

By the invariance principle, all of the solutions of Eq. (12) with the control (28) converge to the largest invariant set in which

$$\langle p_{\dot{r}}, (\delta_k + i) e^{i\gamma_k} \rangle \equiv 0 \tag{30}$$

In this set, $\dot{\gamma}_k = 0$ and $\dot{s}_k = 0$, which implies $p_{\dot{r}}$ is constant. Since $\delta_k + i \neq 0$ (δ_k is real), then the invariance condition (30) is satisfied for all $k = 1, \ldots, N$, only when $p_{\dot{r}} = 0$. □

IV. Stabilization of Circular Formations

In this section, we describe a decentralized algorithm to stabilize a circular formation in which all particles orbit an inertially fixed point at a fixed radius. The center of the circular formation can be prescribed by introducing a virtual particle, as described next. These results represent a direct extension of the flow-free framework [5] to the particle model (12).

In the absence of flow, that is, using the model (1), setting u_k equal to a constant, $\omega_0 \neq 0$, drives particle k around a circle of radius ω_0^{-1} and fixed center [5]

$$c_k \triangleq r_k + \omega_0^{-1} i \frac{\dot{r}_k}{|\dot{r}_k|} \tag{31}$$

In the presence of a time-invariant flowfield, we have the following result [10].

Lemma 1: The model (12) with the control

$$\nu_k = \omega_0 s_k \tag{32}$$

drives particle k around a circle of radius ω_0^{-1} centered at $c_k(t) = r_k(0) + \omega_0^{-1} i e^{i\gamma_k(0)}$.

Proof: We derive the control ν_k that steers the particle around a circle by differentiating Eq. (31) along solutions of Eq. (12). This results in

$$\dot{c}_k = s_k e^{i\gamma_k} - \omega_0^{-1} e^{i\gamma_k} \nu_k = (s_k - \omega_0^{-1} \nu_k) e^{i\gamma_k} \tag{33}$$

Substituting Eq. (32) into Eq. (33) yields $\dot{c}_k = 0$, which proves that the center of the circle is fixed. To complete the proof, we observe that the radius of the circle is $|c_k(t) - r_k(0)| = \omega_0^{-1}$. □

A circular formation is a solution of the particle model (12) in which all of the particles orbit the same circle in the same direction. Let $\mathbf{1} \triangleq (1, \ldots, 1)^T \in \mathbb{R}^N$. In a circular formation, $c_k = c_j$ for all pairs j and k, which implies that a circular formation satisfies the condition $P\boldsymbol{c} = 0$ [5], where P is an $N \times N$ projection matrix given by

$$P = \text{diag}\{\mathbf{1}\} - \frac{1}{N} \mathbf{1}\mathbf{1}^T \tag{34}$$

Note, P projects an element of $\mathbb{C}^N$ into the subspace complementary to the span of $\mathbf{1}$.

We derive a decentralized control that stabilizes a circular formation by considering the potential [5]

$$S(\boldsymbol{r},\boldsymbol{\gamma}) \triangleq \tfrac{1}{2}\langle \boldsymbol{c}, P\boldsymbol{c}\rangle \tag{35}$$

Note $S \geq 0$, with equality only when $\boldsymbol{c} = c_0\mathbf{1}$, $c_0 \in \mathbb{C}$. The time derivative of S along solutions of Eq. (12) is

$$\dot{S} = \sum_{j=1}^{N}\langle \dot{c}_j, P_j\boldsymbol{c}\rangle = \sum_{j=1}^{N}\langle e^{i\gamma_j}, P_j\boldsymbol{c}\rangle(s_j - \omega_0^{-1}v_j) \tag{36}$$

where P_k denotes the kth row of the matrix P. The following result provides a control algorithm to stabilize a circular formation in a time-invariant flow [10]. It extends [5], Theorem 2, which provides a circular-formation algorithm for the flow-free particle model.

Theorem 3: All solutions of the particle model (12) with the control

$$v_k = \omega_0(s_k + K\langle P_k\boldsymbol{c}, e^{i\gamma_k}\rangle), \qquad K > 0 \tag{37}$$

converge to a circular formation with radius ω_0^{-1} and direction determined by the sign of ω_0.

Proof: The potential $S(\boldsymbol{r},\boldsymbol{\gamma})$ is positive definite and proper in the space of relative circle centers. Substituting Eq. (37) into Eq. (36) yields

$$\dot{S} = -K\sum_{j=1}^{N}\langle P_k\boldsymbol{c}, e^{i\gamma_k}\rangle^2 \leq 0$$

By the invariance principle, all of the solutions of Eq. (12) with control (37) converge to the largest invariant set Λ, in which

$$\langle P_k\boldsymbol{c}, e^{i\gamma_k}\rangle \equiv 0 \tag{38}$$

In this set, $\dot{\gamma}_k = \omega_0 s_k$ and $\dot{c}_k = 0$. Therefore, to satisfy the invariance condition (38), all of the solutions in Λ must satisfy $P\boldsymbol{c} = 0$, which is the circular-formation condition. Application of Lemma 1 completes the proof. □

We illustrate Theorem 3 in Fig. 4. The nonuniform flow is generated by Eq. (19) with $a_0 = -0.75$, $\omega = 5/360$, and $\varphi_0 = 8$.

The control algorithm described in Theorem 3 depends not on absolute positions but on *relative* positions, that is, $r_k - r_j$, for any pair k and j. Consequently, the algorithm preserves the symmetry of the closed-loop particle model (12) that renders the model invariant to rigid translation of all of the particles [2]. This property of the control algorithm implies the steady-state center of the circle depends only on initial conditions. For applications in path planning for autonomous vehicles, there exists the need to specify the steady-state center of the vehicle formation in the presence of flow. This need also arises in the context of tracking a target moving at a constant velocity. We describe next a symmetry-breaking algorithm that provides this capability [10].

Following the flow-free development [6], we introduce a virtual particle labeled with $k = 0$ that serves as a reference. The virtual particle dynamics,

$$\dot{r}_0 = s_0 e^{i\gamma_0} \qquad \dot{\gamma}_0 = \omega_0 s_0 \tag{39}$$

where $\omega_0 \neq 0$, are independent of the dynamics of the particles. In the solution to Eq. (39), particle 0 orbits a circle of radius $|\omega_0|^{-1}$ with fixed center $c_0 = r_0(0) + \omega_0^{-1} i e^{i\gamma_0(0)}$. Assume the virtual particle's relative state variables are available to a nonempty subset of the particles, which we call the informed particles. Let $a_{k0} = 1$ if particle k is an informed particle and $a_{k0} = 0$ otherwise.

Consider augmenting the potential S defined in Eq. (35) with the quadratic potential [6]

$$S_0(\boldsymbol{r},\boldsymbol{\gamma}) = \frac{1}{2}\sum_{j=1}^{N} a_{j0}|c_j - c_0|^2$$

which is minimized when $c_j = c_0$ for all $\{j \mid j \in 1,\ldots,N, a_{j0} = 1\}$. The time derivative of $\tilde{S}(\boldsymbol{r},\boldsymbol{\gamma}) \triangleq S(\boldsymbol{r},\boldsymbol{\gamma}) + S_0(\boldsymbol{r},\boldsymbol{\gamma})$ along solutions of Eq. (12) is

$$\dot{\tilde{S}} = \sum_{j=1}^{N}(\langle e^{i\gamma_j}, P_j\boldsymbol{c}\rangle + a_{j0}\langle e^{i\gamma_j}, c_j - c_0\rangle)(s_j - \omega_0^{-1}v_j) \tag{40}$$

This analysis leads to the following corollary to Theorem 3 [10].

Corollary 1: Let $c_0 = r_0(0) + \omega_0^{-1} i e^{i\gamma_0(0)}$ be the fixed reference provided by a virtual particle, $k = 0$, whose dynamics are given by Eq. (39). Let $a_{k0} = 1$ if particle k is informed of the reference and $a_{k0} = 0$ otherwise. If there is at least one informed particle, then all solutions of the particle model (12) with the control

$$v_k = \omega_0[s_k + K(\langle e^{i\gamma_k}, P_k\boldsymbol{c}\rangle + a_{k0}\langle e^{i\gamma_k}, c_k - c_0\rangle)], \qquad K > 0 \tag{41}$$

converge to a circular formation centered at c_0 with radius ω_0^{-1} and direction determined by the sign of ω_0.

Proof: With the control (41), the time derivative of the augmented potential $\tilde{S}(\boldsymbol{r},\boldsymbol{\gamma})$ satisfies

$$\dot{\tilde{S}} = -K\sum_{j=1}^{N}(\langle e^{i\gamma_k}, P_k\boldsymbol{c}\rangle + a_{k0}\langle e^{i\gamma_k}, c_k - c_0\rangle)^2 \leq 0$$

By the invariance principle, all solutions converge to the largest invariant set for which

$$\langle e^{i\gamma_k}, P_k\boldsymbol{c}\rangle + a_{k0}\langle e^{i\gamma_k}, c_k - c_0\rangle \equiv 0 \tag{42}$$

for $k = 1,\ldots,N$. In this set, $\dot{\gamma}_k = \omega_0 s_k$ and $\dot{c}_k = 0$.

If $a_{k0} = 0$ for at least one but not all $k \in \{1,\ldots,N\}$, then the invariance condition (42) is satisfied only if $P_k\boldsymbol{c} = 0$. This implies $\boldsymbol{c}$ is in the span of $\mathbf{1}$, that is, $c_k = c_j$ for all pairs k and j. For all k with $a_{k0} = 1$, the invariance condition becomes

$$\langle e^{i\gamma_k}, c_k - c_0\rangle \equiv 0$$

which holds only if $c_k = c_0$. This implies $c_k = c_0\mathbf{1}$.

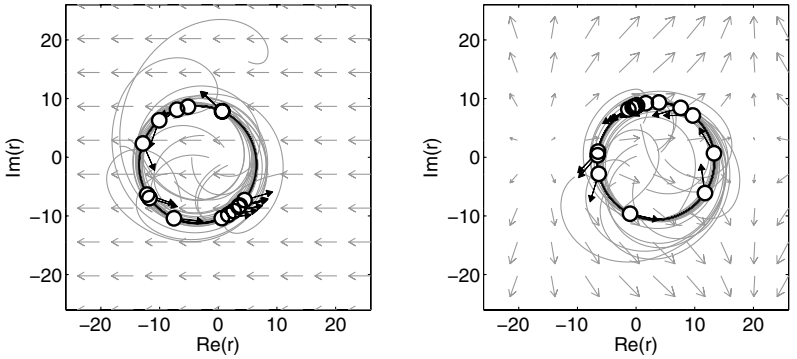

a) Uniform flow, β=−0.75 **b) Nonuniform flow in Eq. (19)**

Fig. 4 Stabilization of a circular formation using control (37) with $N = 15$ and $K = 0.1$.

If $a_{k0} = 1$ for all k, then the invariance condition becomes

$$\langle e^{i\gamma_k}, \tilde{P}_k \boldsymbol{c}\rangle \equiv 0, \tag{43}$$

where $\tilde{P}$ is the $(N+1)\times(N+1)$ projection matrix defined as in Eq. (34). The condition (43) is satisfied only if $c_k = c_0$ for all k, which completes the proof. □

Corollary 1 also provides a procedure to stabilize a circular formation centered on a target moving at a constant velocity. Let $\mathcal{B}$ represent a reference frame that is not rotating with respect to the inertial frame $\mathcal{I}$ and whose origin O' is moving relative to O at a constant velocity b_0 equal to the target velocity. Note that $\mathcal{B}$ is an inertial frame and the target position is a fixed point in $\mathcal{B}$. Let r'_k denote the position of particle k relative to O'. We have

$$\dot{r}'_k = e^{i\theta_k} + f_k - b_0 \tag{44}$$

The equations of motion expressed in frame $\mathcal{B}$ are

$$\dot{r}'_k = e^{i\theta_k} + f'_k \qquad \dot{\theta}_k = u_k \tag{45}$$

where $f'_k \triangleq f_k - b_0$. Therefore, the particle dynamics in frame $\mathcal{B}$ are equivalent to Eq. (12) with r_k replaced by r'_k and f_k replaced by f'_k. Applying the control (41) with c_0 equal to the target position in frame $\mathcal{B}$ stabilizes a circular formation centered on the target. We illustrate this result in Sec. VI.

V. Symmetric Circular Formations

In this section, we provide an algorithm to steer a particle collective to a circular formation and, simultaneously, to regulate the separation of the particles around the circle. To do this, we introduce a phase variable that represents the progress of a particle around the circle [23]. The development of Lyapunov-based algorithms using a phase variable to stabilize symmetric formations is a direct extension of the flow-free framework [5]. In previous work, control laws are provided to regulate the along-track separation of the particles in the absence of flow; here, we provide a control algorithm to regulate the temporal separation of particles in a uniform flowfield.

Recall from Example 1 that the speed of a particle in uniform flow is independent of the particle position, that is, $s_k = s(\gamma_k)$ for all $k = 1, \ldots, N$. According to Lemma 1, the closed-loop phase dynamics

$$\dot{\gamma}_k = \omega_0 s_k \tag{46}$$

drive particle k around a circular trajectory. Integrating Eq. (46) by separation of variables, we obtain

$$t = \frac{1}{\omega_0}\int_0^{\gamma_k(t)} \frac{\mathrm{d}\gamma}{s(\gamma)} \tag{47}$$

which is an implicit expression for the solution to Eq. (46), $\gamma_k(t)$.

The key observation is that we can use a quantity proportional to the right-hand side of Eq. (47) as a measure of the *temporal* separation of solutions to Eq. (46). We call this quantity the time phase ψ_k, defined by [11]

$$\psi_k = \frac{2\pi}{\omega_0 T}\int_0^{\gamma_k} \frac{\mathrm{d}\gamma}{s(\gamma)} \tag{48}$$

where $T > 0$ is the period of a single revolution,

$$T = \frac{1}{\omega_0}\int_0^{2\pi} \frac{\mathrm{d}\gamma}{s(\gamma)} \tag{49}$$

(A similar quantity, called the curve phase, has previously been used to measure arc-length separation along a closed curve [4,23].) The function $\gamma_k = \gamma_k(\psi_k)$ implicitly defined in Eq. (48) is a diffeomorphism, as long as $s(\gamma) > 0$.

We now incorporate the time-phase variable into the design of a formation control. The time derivative of Eq. (48) along solutions of Eq. (12) is

$$\dot{\psi}_k = \frac{2\pi}{T}(\omega_0 s_k)^{-1} \nu_k \tag{50}$$

Let $U(\boldsymbol{\psi})$ represent a smooth potential that satisfies $U(\boldsymbol{\psi} + \psi_0 \mathbf{1}) = U(\boldsymbol{\psi})$, which is the condition for rotational symmetry. Rotational symmetry implies [5]

$$\sum_{j=1}^{N} \frac{\partial U}{\partial \psi_j} = 0$$

Consider the composite potential

$$V(\boldsymbol{r}, \boldsymbol{\gamma}) = S(\boldsymbol{r}, \boldsymbol{\gamma}) + \frac{T}{2\pi} U(\boldsymbol{\psi})$$

where $S(\boldsymbol{r}, \boldsymbol{\gamma})$ is the circular-formation Lyapunov potential defined in Eq. (35). Using Eq. (50) and the rotational symmetry of $U(\boldsymbol{\psi})$, we find

$$\begin{aligned}\dot{V} &= \sum_{j=1}^{N} \langle e^{i\gamma_j}, P_j \boldsymbol{c}\rangle (s_j - \omega_0^{-1}\nu_j) + \frac{T}{2\pi}\frac{\partial U}{\partial \psi_j}\dot{\psi}_j \\ &= \sum_{j=1}^{N} \left(s_j \langle e^{i\gamma_j}, P_j \boldsymbol{c}\rangle - \frac{\partial U}{\partial \psi_j}\right)[1 - (\omega_0 s_j)^{-1}\nu_j]\end{aligned} \tag{51}$$

Choosing the control law

$$\nu_k = \omega_0 s_k \left[1 + K\left(s_j \langle e^{i\gamma_k}, P_k \boldsymbol{c}\rangle - \frac{\partial U}{\partial \psi_k}\right)\right], \qquad K > 0 \tag{52}$$

yields

$$\dot{S} = -K\sum_{j=1}^{N} (s_j - \omega_0^{-1}\nu_j)^2 \le 0$$

and

$$\dot{S} = 0 \Leftrightarrow \nu_k = \omega_0 s_k$$

The following result is obtained using the invariance principle [5].

Theorem 4: Consider the particle model (12) with uniform flow $f_k = \beta$ and a smooth, rotationally symmetric phase potential $U(\boldsymbol{\psi})$. The control law (52) enforces convergence of all solutions to the set of circular formations where all particles move around a circle of radius ω_0^{-1} and direction given by the sign of ω_0 with a phase arrangement in the critical set of $U(\boldsymbol{\psi})$. Every isolated minimum of $U(\boldsymbol{\psi})$ defines an asymptotically stable set of circular formations. Every circular formation where $U(\boldsymbol{\psi})$ does not reach a minimum is unstable.

Proof: See [5], Theorem 3. □

As an example, we describe a phase potential $U(\boldsymbol{\psi})$ that isolates symmetric patterns of the time-phase variables $\boldsymbol{\psi}$. An (M, N) pattern, where M is a divisor of N, is a symmetric arrangement of N phases consisting of M clusters uniformly spaced around the unit circle, each with N/M synchronized phases [5]. For any N, there exist at least two symmetric patterns: the $(1, N)$ pattern, which is the synchronized state, and the (N, N) pattern (the splay state) characterized by N phases uniformly spaced around the unit circle. In a splay pattern of time-phase variables, the particles are uniformly separated in time as they orbit a circular formation in a flowfield. For example, a time-splay configuration in which the particles are labeled sequentially around the formation satisfies [20]

$$\begin{aligned}\gamma_k(t) &= \gamma_{k+1}(t - T/N), \qquad k = 1, \ldots, N-1 \\ \gamma_N(t) &= \gamma_1(t - T/N)\end{aligned} \tag{53}$$

where T is the period of revolution defined in Eq. (49). This type of formation has been explored previously in the context of the particle model (12) [11,20], although we are not aware of any other algorithm proven to force convergence to a time-splay formation. Note, in our

framework, we do not impose the requirement of sequential labeling nor do we require control of particle speed.

Theorem 5: ([5], Theorem 6) Let $1 \leq M \leq N$ be a divisor of N. Then $\boldsymbol{\psi} \in T^N$ is an (M,N) pattern if and only if it is a global minimum of the potential

$$U^{M,N}(\boldsymbol{\psi}) = \sum_{m=1}^{M} K_m U_m \tag{54}$$

with $K_m > 0$ for $m = 1, \ldots, M-1$ and $K_M < 0$, where

$$U_m(\boldsymbol{\psi}) = \frac{N}{2}|p_{m\psi}|^2, \qquad p_{m\psi} \triangleq \frac{1}{mN}\sum_{j=1}^{N} e^{im\psi_j}$$

Note the potential Eq. (54) requires all-to-all communication between the particles to compute the control law (52). An alternate potential (for which (M,N) patterns are also critical points) is available for undirected and connected communication topologies [6]. This potential is a quadratic form that depends on the Laplacian matrix of the communication graph. For example, we illustrate in Fig. 5a a numerical simulation of the feedback stabilization of a time-splay formation using an undirected-ring communication topology. The splay pattern of time phases $\boldsymbol{\psi}$ corresponds to a regular pattern of particle phases $\boldsymbol{\gamma}$ in which sequential particle phases are uniformly separated in time.

The following result provides an algorithm to stabilize a symmetric circular formation at a prescribed reference position. And, following the same procedure described at the end of Sec. IV, it also provides an algorithm to stabilize a symmetric circular formation centered on a moving target, provided the target is moving with constant velocity.

Corollary 2: Let $c_0 = r_0(0) + \omega_0^{-1} i e^{i\gamma_0(0)}$ be the fixed reference provided by a virtual particle, $k = 0$, whose dynamics are given by Eq. (39). Let $a_{k0} = 1$ if particle k is informed of the reference and $a_{k0} = 0$ otherwise. If there is at least one informed particle, then all solutions of the particle model (12) with the control

$$v_k = \omega_0 s_k \left[1 + K\left(s_j\langle e^{i\gamma_k}, P_k \boldsymbol{c}\rangle + a_{k0}\langle e^{i\gamma_k}, c_k - c_0\rangle - \frac{\partial U}{\partial \psi_k}\right)\right] \qquad K > 0 \tag{55}$$

converge to a circular formation centered at c_0 with radius ω_0^{-1} and direction determined by the sign of ω_0. Every isolated minimum of $U(\boldsymbol{\psi})$ defines an asymptotically stable set of circular formations. Every circular formation where $U(\boldsymbol{\psi})$ does not reach a minimum is unstable.

We illustrate Corollary 2 in Fig. 5b.

VI. Application Examples

To demonstrate the utility of the cooperative-control algorithms presented in the preceding sections, we describe two numerical simulations related to applications in environmental monitoring and target surveillance. In the first example, we illustrate a strategy to coordinate multiple aerial vehicles such as the Aerosonde [24] in a simple model of a hurricane. An unmanned aircraft can observe a hurricane at a lower altitude than it is safe to fly a manned aircraft, and therefore presents an attractive option for improving hurricane forecasts via in situ observations. In the second example, we illustrate how multiple aerial vehicles might converge to a time-splay formation centered on a maneuvering target, as long as the target velocity is piecewise constant. This example provides an algorithm for coordinated tracking of a ground target in wind and without speed control. Such an algorithm is suitable for aerial surveillance/reconnaissance missions in which multiple sensing platforms must be coordinated. Each set of numerical results shows convergence of the closed-loop dynamics, despite the fact that theoretical restrictions on flow speed and time invariance are not enforced.

A. Stabilization of a Circular Formation in a Simple Hurricane Model

In this example, we consider the problem of stabilizing a circular formation in the eyewall of a hurricane, where the wind speed vastly exceeds the platform speed. As a simple hurricane model, we use a modified Rankine vortex in which the tangential wind speed v varies with radius r according to two parameters: the maximum wind speed v_m and the radius r_m, at which the maximum wind speed occurs. For $0 < r < r_m$, the wind profile is given by $v(r) = v_m(r/r_m)$; for $r \geq r_m$, $v(r) = v_m(r/r_m)^{-0.6}$. We simulate the particle model (12) with a Rankine vortex located at the origin with $v_m = 3$ (assuming unit particle speed relative to the flow) and $r_m = 1/(2\omega_0)$. Figure 6a illustrates the numerical results for the control (37), which stabilizes a circular formation at an arbitrary center position. Figure 6b illustrates the numerical results for the control (41), which stabilizes a circular formation centered on the vortex. This example illustrates an algorithm for coordinating hurricane observing platforms and suggests that the theoretical results may apply in flowfields whose magnitude exceeds the speed of the particle relative to the flow.

B. Stabilization of a Time-Splay Formation Centered on a Moving Target

In this example, we consider the problem of stabilizing a time-splay formation of aerial vehicles centered on a moving target in the presence of a uniform flowfield. We assume that the target moves with constant velocity between maneuvers. According to the discussion at the end of Sec. IV, we can use as an inertial frame a nonrotating reference frame fixed to the target. We establish such a frame for each constant-velocity portion of the target's trajectory. We simulate the particle model (45) with effective flow speed $f'_k = f_k - b_0$, where the flowfield is $f_k = -0.5$ and the target velocity is $b_0 = \pm 0.25 + 0.25i$ (assuming unit vehicle speed relative to the flow). Note that the magnitude of the effective flow is less than the vehicle speed relative to the flow. The target makes a single, 90-deg turn. Figure 7a illustrates the numerical results in an inertial reference frame that is not translating with the target. Figure 7b uses a target-centered frame to illustrate the numerical

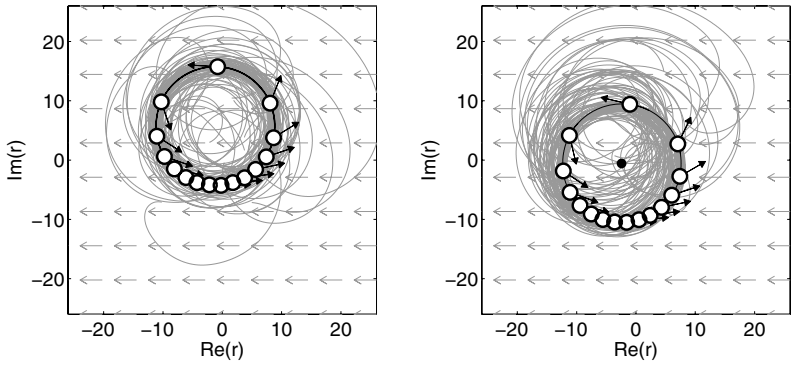

a) Arbitrary center, control (52) **b) Prescribed center, control (55)**

Fig. 5 Stabilization of a time-splay circular formation in uniform flow, $\beta = -0.75$.

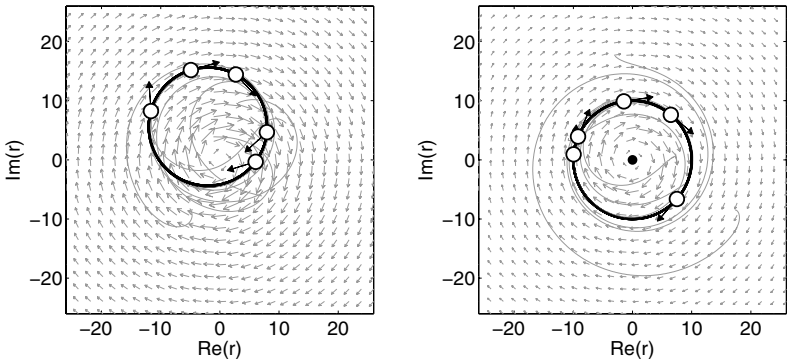

a) Arbitrary center b) Prescribed center

Fig. 6 Stabilization of a circular formation in a simple hurricane model.

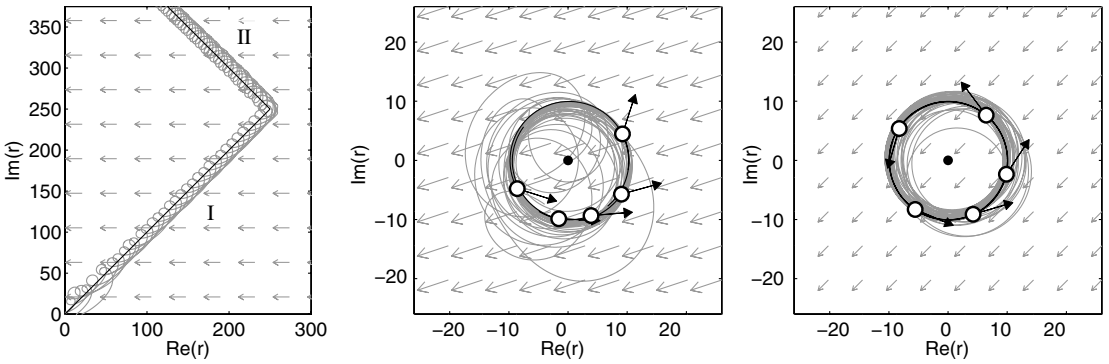

a) Nontranslating frame b) I, target-centered frame c) II, target-centered frame

Fig. 7 Stabilization of a time-splay formation centered on a maneuvering target with piecewise-constant velocity.

results before the maneuver for the control (55), which stabilizes a time-splay formation centered on the target position. Figure 7c illustrates the numerical results in a target-centered frame after the maneuver. The impact of the maneuver can be understood as a step function on the flowfield input. This example provides an algorithm for coordinated tracking of a moving target and suggests that the theoretical results may apply in a flowfield that varies in time.

VII. Conclusions

Distributed sensing with multiple, mobile platforms is enhanced by cooperative-control algorithms that generate coordinated sampling trajectories in the presence of strong and variable flowfields. The design of these algorithms is based on simple models of platform motion that often ignore the presence of flow. In this paper, we describe a self-propelled particle model that explicitly incorporates the presence of a known, time-invariant flowfield. We assume that the flow does not exceed the speed of a particle relative to the flow. We provide decentralized control algorithms that stabilize primitive collection motions including synchronized, balanced, circular, and symmetric circular formations. These motion primitives are essential to the construction of a systematic framework for autonomous and distributed sensing in the presence of flow, as has been illustrated in two numerical examples. In ongoing work, we focus on extending the framework described here to the nonautonomous dynamic systems that arise in the study of time-varying flows.

Acknowledgments

We thank the anonymous reviewers for their insightful comments and suggestions. We also thank Sharan Majumdar for providing the simple hurricane model.

References

[1] Leonard, N. E., Paley, D. A., Lekien, F., Sepulchre, R., Fratantoni, D. M., and Davis, R. E., "Collective Motion, Sensor Networks and Ocean Sampling," *Proceedings of the IEEE*, Vol. 95, No. 1, 2007, pp. 48–74. doi:10.1109/JPROC.2006.887295

[2] Justh, E. W., and Krishnaprasad, P. S., "A Simple Control Law for UAV Formation Flying," [Online] Inst. for Systems Research, Univ. of Maryland, TR 2002-38, 2002, http://www.lib.umd.edu/drum/bitstream/1903/6274/1/TR_2002-38.pdf.

[3] Justh, E. W., and Krishnaprasad, P. S., "Equilibria and Steering Laws for Planar Formations," *Systems and Control Letters*, Vol. 52, No. 1, 2004, pp. 25–38. doi:10.1016/j.sysconle.2003.10.004

[4] Zhang, F., and Leonard, N. E., "Coordinated Patterns of Unit Speed Particles on a Closed Curve," *Systems and Control Letters*, Vol. 56, No. 6, 2007, pp. 397–407. doi:10.1016/j.sysconle.2006.10.027

[5] Sepulchre, R., Paley, D. A., and Leonard, N. E., "Stabilization of Planar Collective Motion: All-to-All Communication," *IEEE Transactions on Automatic Control*, Vol. 52, No. 5, 2007, pp. 811–824. doi:10.1109/TAC.2007.898077

[6] Sepulchre, R., Paley, D. A., and Leonard, N. E., "Stabilization of Planar Collective Motion with Limited Communication," *IEEE Transactions on Automatic Control*, Vol. 53, No. 3, 2008, pp. 706–719. doi:10.1109/TAC.2008.919857

[7] Zhang, F., Fratantoni, D. M., Paley, D. A., Lund, J. M., and Leonard, N. E., "Control of Coordinated Patterns for Ocean Sampling," *International Journal of Control*, Vol. 80, No. 7, 2007, pp. 1186–1199. doi:10.1080/00207170701222947

[8] Paley, D. A., Zhang, F., and Leonard, N. E., "Cooperative Control for Ocean Sampling: The Glider Coordinated Control System," *IEEE Transactions on Control Systems Technology*, Vol. 16, No. 4, 2008, pp. 735–744. doi:10.1109/TCST.2007.912238

[9] Paley, D. A., "Cooperative Control of Collective Motion for Ocean Sampling with Autonomous Vehicles" [Online], Ph.D. Dissertation, Princeton Univ., Princeton, NJ, Sept. 2007, http://wam.umd.edu/~dpaley/papers/paley-thesis.pdf.

[10] Paley, D. A., "Stabilization of Collective Motion in a Uniform and Constant Flow Field," *Proceedings of the AIAA Guidance, Navigation and Control Conference and Exhibit*, AIAA Paper 2008-7173, Aug. 2008, p. 8.

[11] Paley, D. A., "Cooperative Control of an Autonomous Sampling Network in an External Flow Field," *Proceedings of the 47th IEEE*

Conference Decision and Control, Invited Session on "Autonomous Exploration and Remote Sensing," Inst. of Electrical and Electronics Engineers, New York, Dec. 2008, pp. 3095–3100.

[12] Techy, L., Paley, D. A., and Woolsey, C. A.,UAV "Coordination on Convex Curves in Wind: An Environmental Sampling Application," (submitted to European Control Conference 2009).

[13] Ceccarelli, N., Enright, J. J., Frazzoli, E., Rasmussen, S. J., and Schumacher, C. J., "Micro UAV Path Planning for Reconnaissance in Wind," *Proceedings of the 2007 American Control Conference*, American Automatic Control Council, Evanston, IL, July 2007, pp. 5310–5315.

[14] McGee, T. G., Spry, S., and Hedrick, J. K., "Optimal Path Planning in a Constant Wind with a Bounded Turning Rate," *Proceedings of the AIAA Conference Guidance, Navigation, and Control (electronic)*, AIAA Paper 2005-6186, Aug. 2005.

[15] McGee, T. G., and Hedrick, J. K., "Path Planning and Control for Multiple Point Surveillance by an Unmanned Aircraft in Wind," *Proceedings of the 2006 American Control Conference*, American Automatic Control Council, Evanston, IL, June 2006, pp. 4261–4266.

[16] Rysdyk, R., "Course and Heading Changes in Significant Wind," *Journal of Guidance, Control, and Dynamics*, Vol. 30, No. 4, 2007, pp. 1168–1171.
doi:10.2514/1.27359

[17] Techy, L., Woolsey, C. A., and Schmale, D. G., "Path Planning for Efficient UAV Coordination in Aerobiological Sampling Missions," *Proceedings of the 47th IEEE Conference on Decision and Control*, Inst. of Electrical and Electronics Engineers, New York, Dec. 2008, pp. 2814–2819.

[18] Klein, D. J., and Morgansen, K. A., "Controlled Collective Motion for Trajectory Tracking," *Proceedings of the 2006 American Control Conference*, American Automatic Control Council, Evanston, IL, June 2006, pp. 5269–5275.

[19] Rysdyk, R., "Unmanned Aerial Vehicle Path Following for Target Observation in Wind," *Journal of Guidance, Control, and Dynamics*, Vol. 29, No. 5, 2006, pp. 1092–1100.
doi:10.2514/1.19101

[20] Kingston, D. B., "Decentralized Control of Multiple UAVs for Perimeter and Target Surveillance" [Online], Ph.D. Dissertation, Dept. of Electrical and Computer Engineering, Brigham Young Univ., Provo, UT, Dec. 2007, http://www.ee.byu.edu/faculty/beard/papers/thesis/DerekKingstonPhD.pdf.

[21] Frew, E. W., Lawrence, D. A., and Morris, S., "Coordinated Standoff Tracking of Moving Targets Using Lyapunov Guidance Vector Fields," *Journal of Guidance, Control, and Dynamics*, Vol. 31, No. 2, 2008, pp. 290–306.
doi:10.2514/1.30507

[22] Summers, T. H., and Akella, M. R., "Coordinated Standoff Tracking of Moving Targets: Control Laws and Information Architectures," *Proceedings of the AIAA Guidance, Navigation and Control Conference and Exhibit (electronic)*, AIAA Paper 2008-7021, 2008.

[23] Paley, D. A., Leonard, N. E., and Sepulchre, R., "Stabilization of Symmetric Formations to Motion Around Convex Loops," *Systems and Control Letters*, Vol. 57, No. 3, 2008, pp. 209–215.
doi:10.1016/j.sysconle.2007.08.005

[24] Holland, G. J., Webster, P. J., Curry, J. A., Tyrell, G., Gauntlett, D., Brett, G., Becker, J., Hoag, R., and Vaglienti, W., "The Aerosonde Robotic Aircraft: A New Paradigm for Environmental Observations," *Bulletin of the American Meteorological Society*, Vol. 82, No. 5, 2001, pp. 889–901.
doi:10.1175/1520-0477(2001)082<0889:TARAAN>2.3.CO;2